Opto-chemical treatment for enhanced high-level disinfection of mature bacterial biofilm in a Teflon-based endoscope model

Van Nam Tran,[1,5] Periaswamy Sivagnanam Saravana,[2,5] Suhyun Park,[3] Van Gia Truong,[1] Byung-Soo Chun,[2] and Hyun Wook Kang[1,4,*] (ID)

[1] *Industry 4.0 Convergence Bionics Engineering, Pukyong National University, Busan, 48513, Republic of Korea*

[2] *Department of Food Science and Technology, Pukyong National University, Busan 48513, Republic of Korea*

[3] *Department of Electronic and Electrical Engineering, Ewha Womans University, Seoul 03760, Republic of Korea*

[4] *Department of Biomedical Engineering and Marine-integrated Biomedical Technology Center, Pukyong National University, Busan 48513, Republic of Korea*

[5] *These authors contributed equally to this work.*

[*]wkang@pukyong.ac.kr

Abstract: Medical societies and public health agencies rigorously emphasize the importance of adequate disinfection of flexible endoscopes. The aim of this work was to propose a novel opto-chemical disinfection treatment against *Staphylococcus aureus* grown in mature biofilm on Teflon-based endoscope channel models. Laser irradiation using near-infrared and blue wavelengths combined with a low concentration of chemical disinfectant induced both irreversible thermal denaturation and intercellular oxidative stress as a combined mechanism for an augmented antimicrobial effect. The opto-chemical method yielded a 6.7–$\log_{10}$ reduction of the mature *Staphylococcus aureus* biofilms (i.e., approximately 1.0-$\log_{10}$ higher than current requirement of standard treatment). The proposed technique may be a feasible disinfection method for mitigating the risk associated with infection transmission.

1. Introduction

Endoscopy has substantially expanded a variety of procedures by introducing complex instruments into the medical community. More than 17 million gastrointestinal (GI) endoscopies are performed annually in the United States [1,2]. The employed endoscopes are subject to contamination of bacteria, which may cause patient-to-patient infection with use of the instruments [3–6]. The common Gram-positive bacteria are *Staphylococcus aureus* (*S. aureus*) and *Enterococcus faecalis* while Gram-negative microorganisms are *Pseudomonas aeruginosa* (*P. aeruginosa*) and *Escherichia coli (E. coli)*. The rate of infection-related hospitalizations for patients that undergo GI endoscopy within a month was above 104 per 1,000 patients in the United States (~10%) [7]. Thus, the endoscopes must be subjected to a high-level disinfection (HLD) process to meet the safety requirements before their use on the following patient. HLD destroys viruses, vegetative bacteria, fungi, mycobacteria, and some, but not all, bacterial spores [8].

Conventional liquid chemical germicides (LCGs) for HLD, such as glutaraldehyde (GA, concentration of ~2%), ortho-phthalaldehyde (OPA, ~0.55%), peracetic acid (0.23%), and hydrogen peroxide (7.5%) are used to eradicate all mature microorganisms in the endoscope. The current requirement for HLD is defined as the ability to kill 10^6 mycobacteria (i.e., six-log reduction) [9]. Among various LCGs, GA offers numerous benefits to bacterial disinfection in clinics, such as excellent biocidal properties and noncorrosive action to endoscopic equipment,

as it forms protein-protein crosslinks that inhibit protein synthesis [10]. However, its significant inherent limitations include severe irritation to the human respiratory tract, long processing time, protein coagulation, environmental hazard, and high cost [11,12]. HLD using GA has a standard treatment time of ~20 min at 25°C and typically yields 6-$\log_{10}$ reduction of mycobacteria. However, U.S. Food and Drug Administration (FDA) recommends the HLD time of 20~90 min, depending on chemical types. The total estimated cost for reprocessing a typical endoscope is approximately 114~280 USD per endoscope [12,13]. Therefore, alternative solutions are still required to ensure more effective bacterial disinfection during endoscope reprocessing.

Laser irradiation on endoscopes with 808 nm (near-infrared; IR) and 405 nm (blue; BL) wavelengths for antimicrobial purposes paves the way for enhancing bacterial disinfection with both photothermal and photochemical effects [14–16]. In comparison to ultraviolet wavelengths, IR and BL wavelengths are less cytotoxic and easier to deliver through an optical fiber [17]. However, despite emerging antimicrobial methods utilizing laser light, the safe and effective delivery of light into the tubular structure of endoscope working channels (2~4 mm in diameter) is more challenging than that on open surfaces [18]. Moreover, individual treatments of LCG or laser light disinfect biofilms incompletely because the tubular structure of the biofilms is composed of mono- to multi-layers of bacterial cells [19]. Recently, a low concentration of GA combined with laser irradiation (broadband IR and BL) was performed to achieve antibacterial activity on *S. aureus* biofilms with a larger than 6-$\log_{10}$ reduction in the bacterial load *in vitro* [20].

Based on these considerations, the current study examined the potential of a novel opto-chemical treatment with combined antimicrobial effects to eradicate *S. aureus* bacterial biofilm (LCG-resistant bacteria model for endoscope disinfection) often growing in a clinical endoscope [15,21,22]. The internal surface of a Teflon-based endoscope channel model was first exposed to a low concentration of GA solution and then was irradiated by IR and BL wavelengths (sequential treatments). The proposed opto-chemical treatment exhibits an effective technique in disinfecting the bacterial biofilm in the Teflon-based endoscope channel.

2. Materials and methods

2.1. Bacterial biofilm formation

S. aureus biofilm (ATCC 6538) was grown in flexible Teflon channels (inner diameter = 4 mm and outer diameter = 5 mm; Sungjin Co., Seoul, South Korea), emulating a biofilm model formed in an endoscope. The uniform mature biofilm with an aggregation of bacteria living in an extracellular matrix (ECM) was cultured by using a setup (Fig. 1(a)) adapted from the published literatures [23,24]. Initially, the bacteria stock cultures were stored at -80 °C in 20% glycerol. Before experiments, the bacteria were subcultured on the tryptic soy agar (TSA) plate from a frozen stock and incubated at 35 °C. The single colony from the TSA plate was cultivated in tryptic soy broth (TSB) and incubated overnight at 35 °C. The bacterial cell culture was then diluted in fresh TSB (1:100 dilution; equal to optical density of 0.05 at 600 nm) [20]. To begin the culture setup, the bacterial culture broth was supplied to all channels by using a pump (P1: 1.5 ml/min, Shengchen Co., Baoding, China). Then, ten milliliters of the diluted cell cultures were injected into the channel. A second pump (P2: 100 ml/ min, Shengchen Co., Baoding, China) was used to thoroughly agitate the channels before the first pump (P1) was turned on to provide continuous tryptic soy broth (TSB) for 72 h at 35 °C. A digital microscope camera (AM413ZT, Dino-Lite, Taipei, Taiwan) monitored the formation of the multilayered biofilm daily. A crystal violet (CV) staining visualized the formation of the *S. aureus* bacterial biofilm. The channels with mature bacterial biofilms were washed with distilled water three times, then stained with CV for 20 min. The stained biofilm inside the channel was flushed out using 95% ethanol, collected in a 96-well plate, and then measured the optical density at 570 nm by a microplate reader (Multiskan GO, Thermo Fisher Scientific, Waltham, Massachusetts, USA); N = 5 per

condition) [25]. To avoid contamination, the growth system was placed in a biological safety cabinet, and the culturing media was changed every four hours.
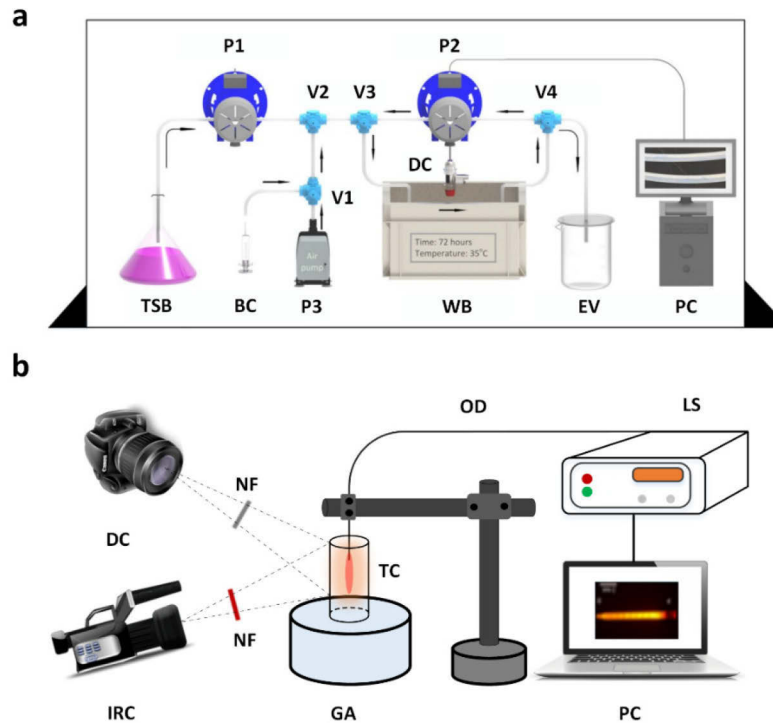
Fig. 1. Schematic illustrations of (a) systematic formation of *S. aureus* biofilm in Teflon channel and (b) experimental set-up for opto-chemical disinfection: biofilms were continuously grown in 72 h at 35 °C. Opto-chemical treatment was conducted in a sequential order of GA immersion, IR, and BL irradiations (P1: media supply pump; P2: agitation pump; P3: air pump; V1, V2, V3, and V4: three-way stopcocks; TSB: tryptic soy broth; BC: bacterial culture; DC: digital camera; WB: water bath; EV: evacuation; PC: personal computer; NF: neutral filter; IRC: infrared camera; GA: glutaraldehyde; TC: Teflon channel; OD: optical diffuser; LS: laser system of IR and BL).

2.2. Optical delivery design

A ray-tracing numerical model was initially developed to simulate distribution of the photons emitted from an optical diffuser by using the Monte Carl program (TracePro, Lambda, MA, USA) and to optimize the design of the diffuser. The model used a 600-μm core optical fiber (NA=0.5; $n_{core} = 1.46$; $n_{cladding} = 1.37$; Thorlabs, USA) with a 10-mm diffusing active segment at the distal end of the fiber. The diffusing surface was assumed to have parallelogram groove patterns (75 μm × 75 μm) to have the total internal reflection at the surface and to yield a cylindrical distribution of high laser power for uniform light diffusion. A million rays of a light source with a Gaussian distribution were coupled into the optical fiber. A planar detector (20 mm × 20 mm) was used to detect the photons emitted from the fiber surface. Based on the simulation results, the optical diffuser was fabricated by micromachining the 600-μm optical fiber tip with a CO_2 laser system [26]. The parallelogram groove patterns were created on the surface of the distal fiber end and were imaged by using scanning electron microscopy (SEM) for qualitative evaluations.

2.3.   Light sources

A customized 10-mm long optical diffuser (TeCure, Inc. Busan, Korea) was used to distribute laser light to the bacterial biofilm on the internal surface of the Teflon channels (Fig. 1(b)) [26]. High-power class IV diode laser systems (CNI laser, Changchun, P.R. China) were used to deliver narrowband wavelengths of IR ($\lambda = 808$ nm; bandwidth = ±3 nm) and BL ($\lambda = 405$ nm; bandwidth = ±5 nm) for all the experiments. The laser systems were operated with a programmable modulator to transmit uniform irradiation to mature biofilm formed in Teflon channels (< 2% of power stability). At each wavelength, a digital camera (Nikon D3500, Nikon Inc., Melville, NY, USA) took images of the light distribution on the inner channel surface. Image J software (National Institutes of Health, Bethesda, Maryland, USA) was used to measure the longitudinal emission profiles from the optical diffuser.

2.4.   Characterization of optical and thermal responses

An end-firing flat fiber delivered IR light on a 1-mm thick Teflon plate (Sungjin Co., Seoul, South Korea) in order to characterize optical and thermal responses of the Teflon to IR irradiation. A power meter (50(150) A-BB-26, Ophir Co., Darmstadt, Germany) was used to measure the transmission power at various power levels. An infrared camera with a spectral range of 7.5-13 μm (A325SC, FLIR, Inc., Wilsonville, Oregon, USA) monitored the spatiotemporal developments of temperature on the Teflon surface to verify any occurrence of thermal damage to the Teflon plate. The Teflon plates were cut into 5 mm × 5 mm, and all the pieces were mounted and sputter-coated with gold-palladium for scanning electron microscopy (SEM; S-3400N, Hitachi, Tokyo, Japan) and further image processing by Image J software.

2.5.   Treatment dosimetry

Upon biofilm preparation, the dosimetry for chemical and optical treatments was examined to identify optimal treatment conditions [20]. Four different concentrations (0.1, 0.5, 1, and 2%) of glutaraldehyde (GA) was tested on each established biofilm channel (10 mm long) for 180 s (N = 5). The current standard concentration (2%) for endoscope disinfection was considered as a Ref. [27]. The optical treatment applied two wavelengths (808 nm for IR at 10 W/cm^2 and 405 nm for BL at 1.6 W/cm^2) for various durations (120, 180, 240, and 300 s; N = 5) [20]. The corresponding fluences for IR were 1200, 1800, 2400, and 3000 J/cm^2, respectively. The fluences for BL were 192, 288, 384, and 480 J/cm^2, respectively. Once the optimal dosage was identified for the chemical and optical treatments, seven different treatment conditions (individual or combined) were examined to investigate antimicrobial effects (individual treatments = GA, IR, and BL and combined treatments = GA + IR, GA + BL, IR + BL, and GA + IR + BL). For the combined treatments, the treatment sequence was maintained in the order of GA, IR, and BL (i.e., GA + IR: GA followed by IR; GA + BL: GA followed by BL; IR + BL: IR followed by BL; and GA + IR + BL: GA followed by IR and then BL), in accordance with our previous study [20].

2.6.   Cell viability

For the quantification of viable bacteria in CFU/cm^2, each 10-mm treated channel was washed with distilled water and put in a 15ml conical tube with 1 ml distilled water. The prepared channel was sonicated for 30 min (frequency = 40kHz), followed by vortexing for 5 min. The bacterial suspension was acquired and diluted ten-fold, then 100 μl of the bacterial suspension was spread on the trypticase soy agar (TSA) plate to aerobically incubate for 24 h at 37 °C. After visually counting the bacterial colonies, we presented all results as the log number of viable bacterial cells in the biofilm from the channel surface (CFU/cm^2; N = 5 per condition).

2.7. Microscopic determination of biofilm architecture and cell membrane integrity

To visualize the biofilm architecture, all treated channels were washed several times with distilled water and fixed using 2.5% GA in 0.1 M phosphate-buffered saline (PBS; pH = 7.2) for 4 h at 4 °C. Then, the treated channels were dehydrated in increasing ethanol concentrations (10, 25, 50, 75, and 100%) for 10 min and isoamyl (100%) for an additional 10 min [20]. The final biofilm channels were cut into 5 mm long pieces for SEM evaluations. MATLAB (R2019b, MathWorks, Natick, MA, USA) was used to analyze and estimate the bacterial coverage after each testing condition. The percentage of residual bacteria surface was calculated from each segmented image (N = 5). A moving window (6×5 µm^2) was applied to calculate the corresponding standard deviation for each SEM image (26×17 µm^2 for $\times$5,000). An image histogram was created to determine the entire tonal distribution in each digital image.

A LIVE/DEAD BacLight Bacterial Viability Kit (Bio Probes Inc., Eugene, OR, USA) was used to visualize the membrane integrity of the treated biofilms. SYTO 9 and PI stains were thoroughly mixed with a ratio of 1: 1. Then, 3 µl of the mixed dye was added to each 1 ml bacterial suspension, which was removed from the biofilm-established channel, and incubated in a dark room for 15 min at room temperature. Five microliters of the stained bacterial suspension were placed between a glass slide and an 18 mm square coverslip for observation under an inverted microscope (CKX53, Olympus, Inc., Tokyo, Japan) (N = 5). As the live bacteria region was colored green, global thresholding in the RGB space was used to segment the green area by using MATLAB. The total biofilm coverage of live bacteria regions was quantified from each segmented fluorescence image. A moving window (40×40 µm^2) was used to estimate the standard deviation for the quantified biofilm coverage (0.31×0.23 mm^2 for $\times$40). A histogram for each image illustrated a graphical representation of the tonal distribution.

2.8. Evaluation of oxidative stress

The degree of oxidative stress generation from seven treatment groups (GA, IR, BL, GA + IR, GA + BL, IR + BL, GA + IR + BL) was examined to explain antimicrobial mechanism. Each 10-mm treated channel was washed with distilled water, placed into a 15 ml conical tube with 1 ml distilled water, sonicated for 30 min (frequency = 40 kHz), and vortexed for 5 min to detach all bacterial biofilm from the channel. A 1 mg nitro blue tetrazolium (NBT) solution was added to the tube after incubation in a dark room for 30 min. To stop the bacterial reaction with NBT, 0.1 M HCl was added to the solution, and all the tubes were centrifuged at 12,000g for 5 min. The separated pellets were treated with 800 µl saline, followed by 400 µl of dimethyl sulfoxide (DMSO) to release intercellular ROS. A 200 µl volume of each sample was placed in a 96-well plate and measured five times at 575 nm by using a microplate reader for the estimation of ROS generation (N = 5 per condition). To eliminate any experimental errors caused by the sonication process, the acquired ROS production was normalized by the absorbance of control samples. The degree of increase (D_i) in intercellular ROS was calculated by the equation:

$$D_i = \frac{A_t - A_c}{A_c} \times 100\%$$

(1)

where A_t and A_c are the absorbance of treated and control samples, respectively.

2.9. Statistical analysis

One control and seven treatment conditions were evaluated on the established biofilm models. Each group was treated five times (N = 5). The results were presented as the mean ± standard deviation (SD). A non-parametric Kruskal-Wallis test was employed to evaluate the differences among the groups due to the small sample size and distribution-free data [28,29]. A Mann-Whitney U test was used to assess the statistical differences between two groups. A Bonferroni

correction with an adjusted *p* value was used as a post hoc test to minimize the chances of incorrectly rejecting the null hypothesis when comparing each pair of the groups. A SPSS program (SPSS, Inc., Chicago, USA) assisted the calculation process, and $p < 0.05$ was regarded as a significant difference.

3. Results

Figure 2 shows the extent of bacterial biofilm formation inside a Teflon channel. After adhesion to the surface, the bacterial biofilm proliferated and fully matured for three days (Fig. 2(a)). The optical density of the multilayered bacterial biofilms for Day 1 and Day 2 was 23.4% and 46.7%, respectively, in comparison to that of Day 3 (Fig. 2(b)).
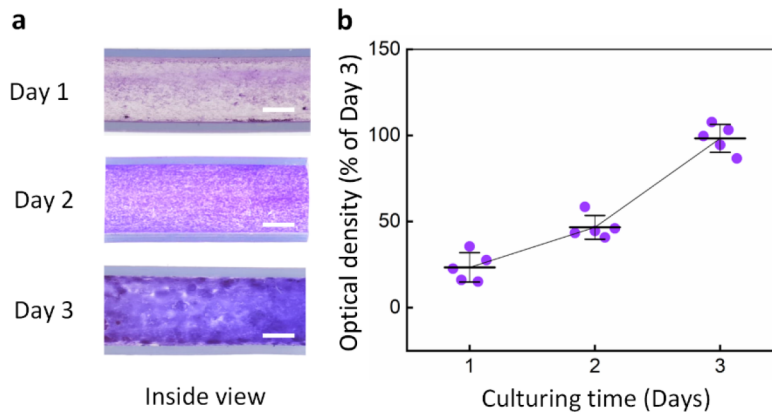

Fig. 2. Formation of *S. aureus* biofilm inside Teflon channel: (a) visualization of biofilm-seeded channel (inner surface) with crystal violet staining and (b) changes in optical density at 570 nm for various culturing times (scale bar = 2 mm).

Optical simulations presented a uniform light distribution within a 10 mm active segment of an optical diffuser tip (Fig. 3(a)). An SEM image confirmed parallelogram grooving patterns (75 μm × 75 μm) on the fiber surface (top; Fig. 3(b)). The fabricated optical diffuser distributed IR and BL lights inside the Teflon channels circumferentially (bottom; Fig. 3(b)). Figure 3(c) compares longitudinal emissions between the simulation (top) and the experiment (bottom). The longitudinal light intensity was normalized by the maximum intensity measured from the optical diffuser. Both the results yielded almost rectangular profiles from the proximal to the distal ends of the diffuser (deviation of ≤ 20%). The simulation generated a symmetrical distribution whereas the experiment had a slightly right-skewed distribution. It is noted that both IR and BL exhibited comparable light distributions along the optical diffuser (Figs. 3(b) and 3(c)).

Figure 4 presents Teflon transmission and temperature development under IR irradiation. The light transmission of a Teflon plate with and without water was 82% and 90% at various power levels, respectively (Fig. 4(a)). The maximum temperature development of the Teflon surface was 54.5 °C and 37.5 °C under irradiance of 10 W/cm^2 for 180 s, respectively (Fig. 4(b)). Moreover, to investigate the energy threshold for thermal damage on the Teflon plate, the laser irradiance was increased to 20 W/cm^2 (Fig. 5). The scanning electron microscopic images and 3D surface profiles showed no physical damage to the surface of both the 0-min (untreated control) and 3-min (treated) samples due to the high melting point (~260 °C) of Teflon (Figs. 5(a) and 5(b)). However, thermal damage on the Teflon surface was observed after 15 min of irradiation (18,000 J/cm^2 and maximum temperature = ~280 °C; Fig. 5(c)). It should be noted that BL exposure yielded a low temperature increase (< 10 °C) of the Teflon plate due to low irradiance (1.6 W/cm^2).
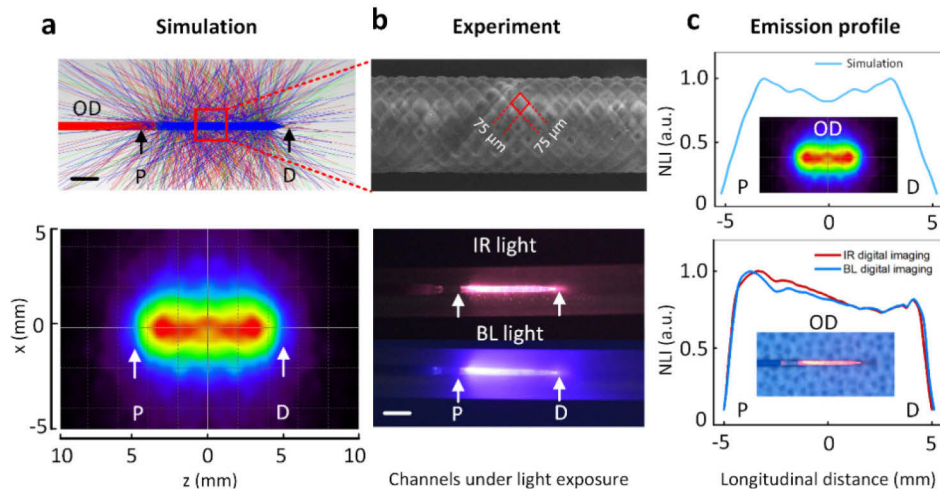
Fig. 3. Simulation and validation of optical diffuser: (a) ray-tracing model (top) and longitudinal emission map (bottom), (b) SEM image of optical diffuser tip (top) and light emission in Teflon-based endoscope channel (bottom), and (c) longitudinal emission profiles acquired by simulation (top) and digital imaging (bottom; normalized light intensity measured from middle of active segment; IR wavelength = 808 nm; BL wavelength = 405 nm; OD = optical diffuser; NLI = normalized light intensity; P = proximal and D = distal ends; scale bar = 2 mm).
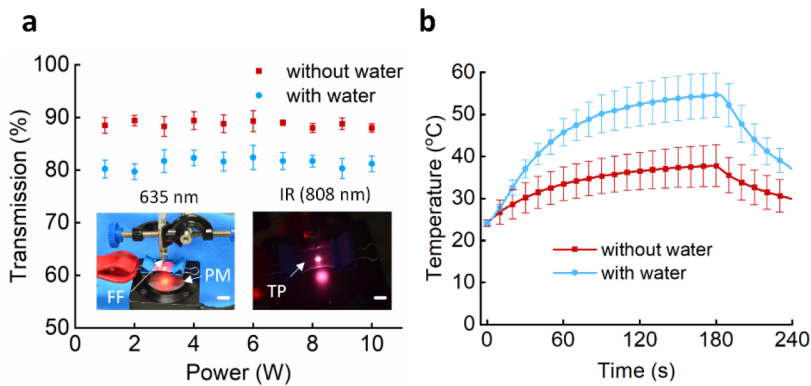

Fig. 4. Characterization of optical and thermal responses of Teflon plate to IR exposure: (a) light transmission of Teflon plate at various power levels (irradiance = 5, 10, 15, 20, 25, 30, 35, 40, 45, and 50 W/cm^2) and (b) temperature development of Teflon surface under irradiance at 10 W/cm^2 for 180 s (FF: end-firing flat fiber; PM: power meter; TP: Teflon plate; scale bar = 5 mm).
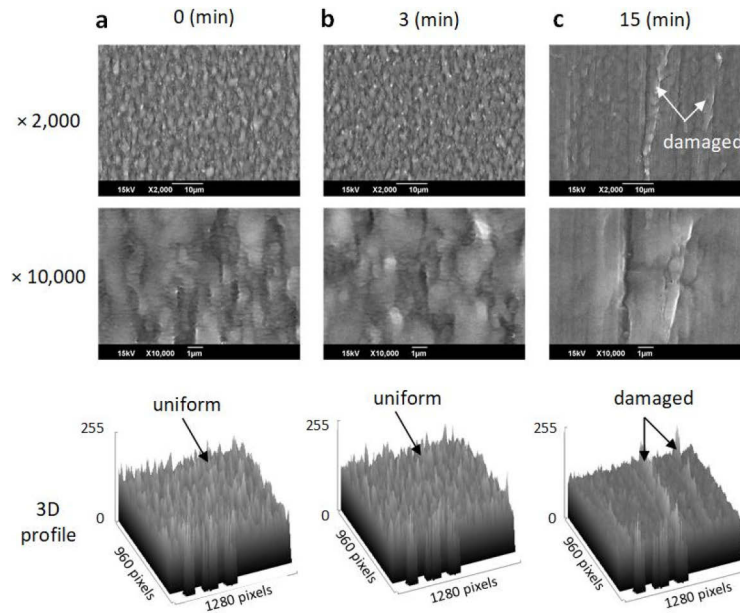
Fig. 5. Qualitative evaluations on surface of Teflon plate after IR (808 nm) irradiation at 20 W/cm^2: (a) no irradiation (control; 0 J), (b) short irradiation for 3 min (3,600 J; maximum temperature = ~55 °C), and (c) long irradiation for 15 min (18,000 J; maximum temperature = ~280 °C). Bottom images show 3D surface profiles of the irradiated channel surfaces.

The reduction in *S. aureus* bacteria biofilms after various individual treatments was quantified to determine the optimal conditions for combined antimicrobial effects (Fig. 6(a)). Irrespective of its concentration, GA treatment significantly reduced the bacterial population of the biofilm, in comparison to the control ($p < 0.01$; Fig. 6(b)). Although the highest concentration yielded the maximum reduction (4.1-log$_{10}$), the rate of bacterial reduction became saturated with increasing GA concentration ($p = 0.32$ for 0.5 vs. 1.0%). A low concentration of GA (0.5%) was then selected for further tests by considering the objective of attaining an environmentally safe disinfection of endoscopes. Both IR and BL exposure reduced the bacterial population in the biofilm ($p < 0.01$ vs. control). BL eradicated the bacterial biofilm in the channel to a greater extent than IR (~40%) for all applied fluences (Fig. 6(c)). Despite achieving the largest reduction (2.8-log$_{10}$ for BL) after the longest irradiation time (300 s), the degree of bacterial eradication became saturated with increasing fluences for both IR and BL ($p = 0.15$ for IR and $p = 0.13$ for BL). Based on the comparable bacterial reduction, the shortest irradiation time of 180 s for IR and BL were selected for further experiments.

Figure 7 presents SEM and fluorescent images on the bacterial biofilms exposed to seven different treatment conditions (GA, IR, BL, GA + IR, GA + BL, IR + BL, and GA + IR + BL). The untreated control displays a large number of bacterial colonies that established a compact biofilm architecture composed of extracellular polymeric substances (Fig. 7(a1)). The opto-chemical condition (GA + IR + BL) significantly reduced the bacterial colonies in the biofilm seeded on a Teflon-based endoscope channel, indicating the absence of intact biofilm morphology ($p < 0.001$ vs. all conditions; Fig. 7(e1)). The individual treatments demonstrated the partial removal of the bacterial density, compared to the untreated control (Figs. 7(a1)~7(d1)). Fluorescent image measurements confirmed that the application of GA + IR + BL markedly reduced the bacterial cell population, exhibiting minimal intact cell membranes (green; Fig. 7(e2)). As the total cell
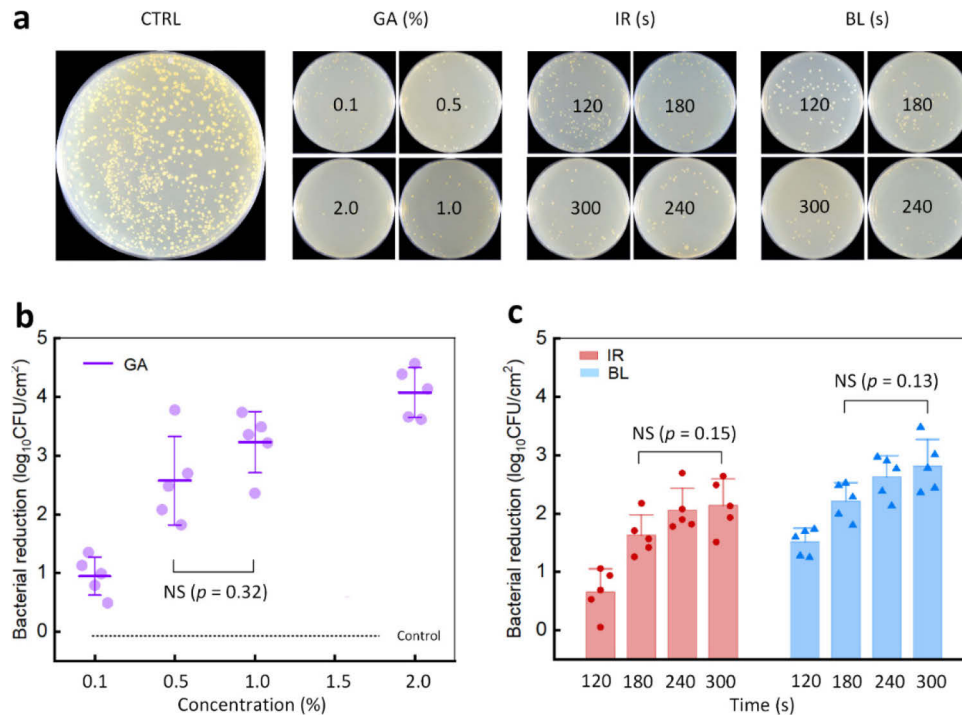
Fig. 6. Determination of *S. aureus* bacterial reduction in CFU under exposure of glutaraldehyde (GA) and laser lights: (a) CFU on agar plates (CTRL = control), (b) GA (concentrations = 0.1, 0.5, 1, 1.5, and 2%), (c) IR and BL (irradiation time = 120, 180, 240, and 300 s). Lines show the mean, dots represent replicates, and error bars indicate standard deviations (CFU: colony forming unit; GA: glutaraldehyde; IR: 808 nm laser light; BL: 405 nm laser light; NS: not significant vs. IR or BL irradiation for 180 s; N = 5).

population was lower than that of the control, propidium iodide stained the remaining dead cells (red) after their detachment from the channel surface resulting from the combined antimicrobial effect (Figs. 7(a2) and 7(e2)). However, a considerable number of bacterial cells were still viable under other treatment conditions (Figs. 7(b2)~7(d2)). The biofilm coverage measured in the SEM images showed a substantial decrease with GA + IR + BL ($p < 0.001$ vs. all conditions; Fig. 7(f1)). The quantification of green intensity, representing live bacterial cells, likewise confirmed that GA + IR + BL led to a minimal number of live cells with a green intensity of 10% ($p < 0.001$ vs. all conditions; Fig. 7(f2)), which agrees well with the results in Fig. 7(f1). The histograms of the biofilm counts measured from SEM and fluorescent images validate that the opto-chemical treatment resulted in a narrow distribution of pixel intensity, in contrast to the wide distribution of the control, representing background images with almost no viable bacterial cells after the GA + IR + BL exposure (Figs. 7(g1) and 7(g2)).

As the antimicrobial activity of BL on *S. aureus* relies on the production of oxidative stress, the extent of ROS increase was initially evaluated for seven different treatment conditions (GA, IR, BL, GA + IR, GA + BL, IR + BL, and GA + IR + BL; Fig. 8(a)). The combination of GA + IR + BL (opto-chemical method) yielded the maximum ROS generation among the tested conditions ($p < 0.01$ vs. GA and $p < 0.05$ vs. BL). The photothermal effect resulting from IR on the irradiated biofilm led to a slight increase in the ROS generation (8.1%; $p < 0.05$ vs. GA). In contrast, BL and its combinations (GA + BL, IR + BL, and GA + IR + BL) yielded marked increases in the intercellular ROS levels (30.6%, 32.0%, 38.1%, and 41.4%, respectively). Therefore, the BL
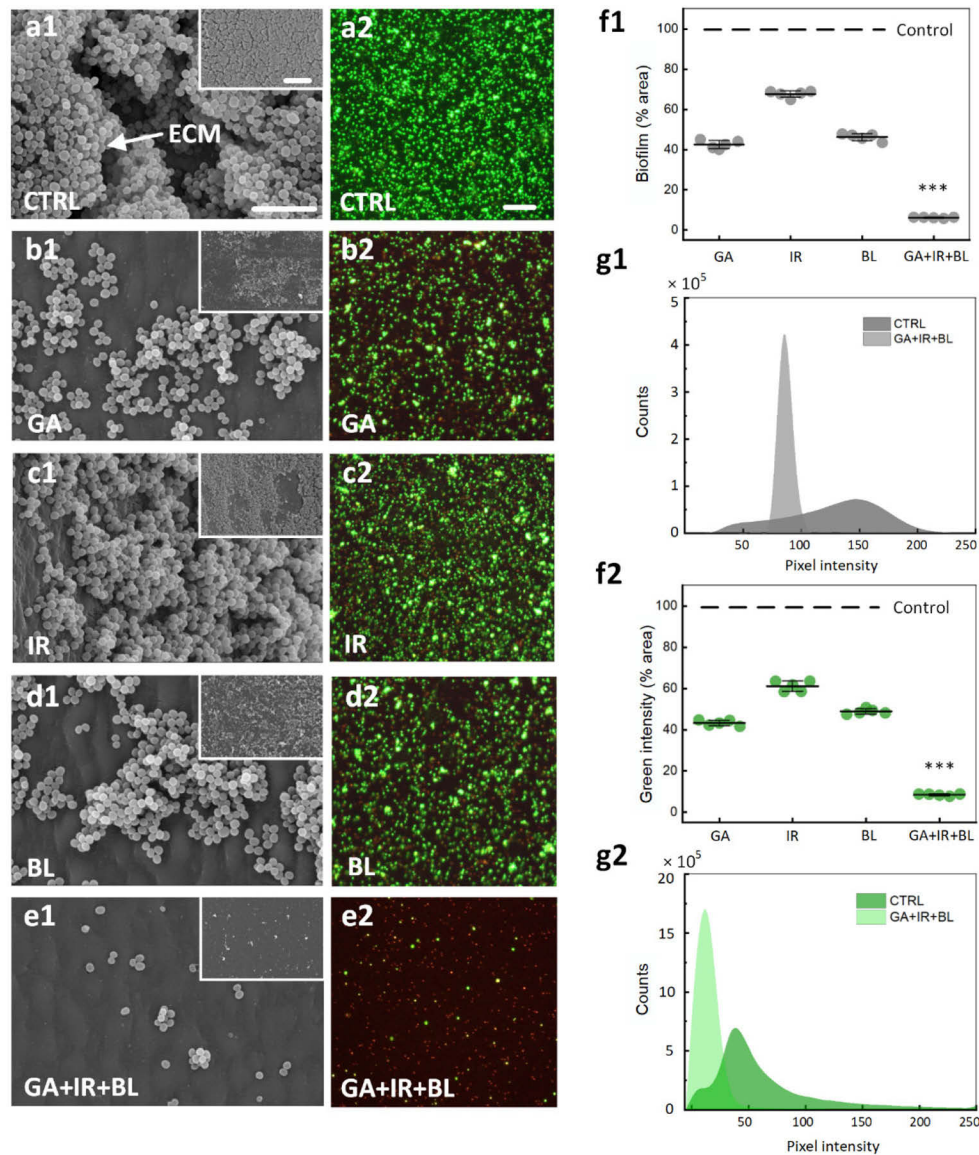
Fig. 7. Scanning electron microscope (SEM; left column) and fluorescent images (right column) of *S. aureus* bacterial biofilm treated after various treatment conditions. (a1 and a2) untreated control (CTRL), (b1 and b2) GA, (c1 and c2) IR, (d1 and d2) BL, and (e1 and e2) GA + IR + BL, (f1) bacterial biofilm coverage and (g1) pixel intensity distributions estimated from SEM images, (f2) green intensity and (g2) pixel intensity distributions estimated from fluorescent images. Live *S. aureus* bacterial cells were stained with SYTO 9 (green); dead bacterial cells were stained with propidium iodide (PI; red). Lines show the mean, dots represent measurement replicates, and error bars indicate standard deviations. (GA concentration = 0.5%; IR and BL irradiation time = 180 s; ECM = extracellular matrix; ***$p < 0.001$ vs. other conditions; magnification = ×5,000 for main SEM images and ×500 for inlets; scale bar = 5 μm for SEM and fluorescent images and 50 μm for inlets; N = 5).

irradiation induced oxidative stress as a dominant mechanism for antimicrobial activity. The opto-chemical method yielded the maximum bacterial reduction (6.7-$\log_{10}$; $p < 0.001$ vs. all conditions; Fig. 8(b)) which is higher than the current disinfection requirement. These combined antimicrobial effects included inhibition of protein synthesis, photothermal effect, and oxidative stress. The top part in Fig. 8(b) represents the temperature increase and ROS generation during the treatments (+: high and −: low). The individual treatments (GA, IR, or BL) achieved
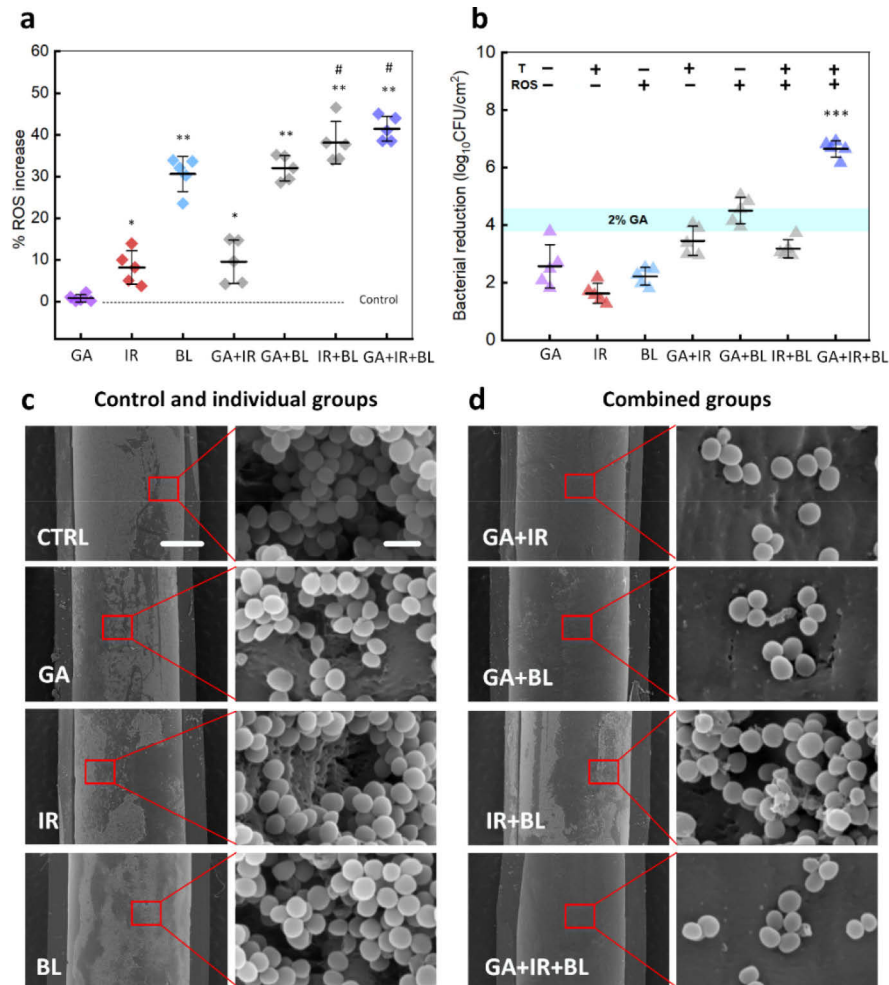
Fig. 8. Effect of opto-chemical treatment on *S. aureus* bacterial biofilm after various treatment conditions. (a) detection of reactive oxygen species (ROS) under seven treatment conditions (GA, IR, BL, GA + IR, GA + BL, IR + BL, and GA + IR + BL, (b) total bacterial reduction under seven treatment conditions (GA concentration = 0.5%; IR and BL irradiation time = 180 s), scanning electron microscope (SEM) images of (c) untreated control and individual treatment groups (CTRL, GA, IR, and BL), and (d) combined treatment groups (GA + IR, GA + BL, IR + BL, and GA + IR + BL; scale bars: left = 1 mm and right = 1 µm; GA concentration = 0.5%; IR and BL irradiation time = 180 s). The top part in (b) shows the level of temperature and ROS (T: temperature; +: high value; -: low value). A cyan line in (b) represents a range of bacterial reduction by standard disinfection with 2% GA. Lines show the mean, dots represent replicates, and error bars indicate standard deviations (*$p < 0.05$ and **$p < 0.01$ vs. GA; ***$p < 0.001$ vs. all other conditions; N = 5).

a comparatively low bacterial eradication in the biofilm due to the individual antibacterial effect. In contrast, once GA was combined with IR or BL, the combinations (GA + IR and GA + BL) led to a moderate reduction in the bacterial population from the inhibition of protein synthesis in conjunction with either a high temperature (GA + IR) or high ROS (GA + BL). Without GA, the treatment with both IR and BL (IR + BL: high temperature and ROS) yielded a slightly lower reduction in the biofilm population than the GA + IR and GA + BL treatments ($p < 0.05$; Fig. 8(b)). These results indicate that protein synthesis in the bacteria must have been inhibited before the dual-antimicrobial activities of IR and BL irradiation was applied on the *S. aureus* biofilm. Subsequently, SEM images confirmed bacterial removal in the biofilm under individual and sequentially combined treatments (Figs. 8(c) and 8(d)). Both individual and dual combinations of treatments demonstrated the partial removal of the bacterial density, compared to the untreated control. However, a considerable number of bacterial cells was eradicated under the opto-chemical treatment (GA + IR + BL; Fig. 8(d); bottom).

4. Discussion

The current study demonstrates the significant capability of the novel opto-chemical treatment strategy to exert an enhanced antimicrobial effect with a lower concentration of GA against an opportunistic respiratory pathogen (*S. aureus*) formed in a flexible endoscope model. While previous research has reported antibacterial effects of individual treatments (GA, IR, or BL) [10,15,22], this study demonstrated the augmented disinfecting efficacy of the combined treatment on mature bacterial biofilm grown in a Teflon-based endoscope model. Due to difficult procurement of clinical flexible endoscopes, the current study developed a culture system to grow a uniform bacterial biofilm in a Teflon-based channel instead to emulate the clinical endoscope (Fig. 2). An optical diffuser was used for the effective delivery of IR and BL lights into a narrow Teflon-based endoscope channel (ID = 4 mm) for HLD testing. An optical ray-tracing program was also used to simulate an optical path and light emissions for comparison with the performance of the fabricated optical diffuser. Thus, the current study was able to customize a flat-top uniform light emission from the optical diffuser (Fig. 3). However, slightly different light emission profiles between simulation and experiment might have resulted from the grooving patterns created on the optical fiber surface [26] (Fig. 3(c)). Therefore, further investigations will be performed to optimize the optical simulations and improve a micromachining system for precise fabrication of the optical diffuser.

  The combined opto-chemical treatment enhances the antimicrobial effect on the mature biofilm. The dominant mechanisms responsible for the combined disinfection are irreversible thermal denaturation and the formation of intercellular ROS, which was validated in previous studies [20]. The presence of the GA solution forms protein-protein crosslinks with hydroxyl, carboxyl, and amino groups both at the membrane and inside the cytoplasm; thereby, it arrests the metabolic process and the GA solution leads to cell death (i.e., inhibition the process of protein and DNA synthesis) [10,30]. In contrast, the irreversible thermal denaturation of the membrane and cell biomolecules (e.g., nucleic acids, proteins, and lipids) resulted from IR light absorption by a combination of the Teflon, water molecules, and bacterial biofilms in the endoscope channel (Fig. 4) [31–34]. Physically, IR light can damage ribosomes and RNA polymerase before disrupting DNA and cell membranes. Furthermore, RNA, protein, and cell membranes exhibited a greater vulnerability to the IR thermal effect [35]. Conversely, endogenous porphyrins in bacterial cells absorbed BL selectively and generated the intracellular ROS that is sufficient to effectively kill the bacteria (Fig. 8(a)), which agrees with a previous study [22]. Rupel *et al.* reported that the overproduction of oxidative stress may cause severe damage to bacterial membranes with multiple blebs [14]. Furthermore, ROS can lead to lipid peroxidation, protein and nucleic acid oxidation, and enzyme inhibition, ultimately causing cell death [36]. In spite of the enhanced antimicrobial effect, the current study merely employed a single sequence (order of GA, IR,

and BL) for the opto-chemical treatment. Therefore, various treatment orders should further be examined to investigate the effect of the treatment sequence on disinfection performance as well as long-term bacterial resistance. Liquid chromatography-tandem mass spectrometry will measure endogenous porphyrins within various bacteria to elucidate the underlying interplay between BL and biofilm disinfection [37]. Exogenous porphyrins (photosensitizer) will also be evaluated with the proposed opto-chemical treatment in order to explore the potential antimicrobial effect against the bacterial biofilm and to provide the alternative agents to conventional LCGs for HLD.

The present study proposes a non-invasive sequential opto-chemical treatment. This method may mitigate the current concerns voiced by medical communities and public health agencies regarding incomplete disinfection of a flexible endoscope to prevent the secondary infection in the clinical situations [38,39]. The use of the sequential opto-chemical disinfection method offers an enhanced antimicrobial effect on contaminated Teflon channels (6.7-$\log_{10}$ bacterial reduction vs. 6-$\log_{10}$ for standard treatment [40]) in a shorter treatment time (9 min vs 20 min for standard treatment). Moreover, the application of a lower concentration (0.5% vs. 2% for standard treatment) can help diminish chemical use, cost, and hazardous effect on health and environment. However, the proposed opto-chemical treatment still requires additional laser systems and delivery device that may increase the total treatment cost. A number of studies have been performed to disinfect the bacterial biofilm. Neves *et al.* reported that application of 2% GA for 20 min, 0.15% peracetic acid for 10 min, or OPA solution was able to disinfect 5-$\log_{10}$ of *S. aureus* or *P. aeruginosa* bacterial populations grown on the inner surface of endoscope channels [41]. Balsamo *et al.* performed different disinfection methods on Teflon channels by using 2% GA (both manual and automated techniques) and peracetic acid (0.15% for manual and 35% for automated manners). However, none of the disinfection techniques completely eradicated the *P. aeruginosa* bacterial biofilm [42]. Bhatt *et al.* recently proposed a low-temperature plasma-activated gas treatment against the biofilm on the contaminated endoscope channels. The technique achieved dispersal of *S. aureus*, *P. aeruginosa*, or *E. coli* bacterial biofilm in 9 min without regrowth, which is comparable to the current findings [39]. Therefore, further studies will be performed to investigate the simultaneous opto-chemical treatment, which could be more effective than the sequential method in warranting the safety margin of the current HLD process. IR (10 W/cm^2) and BL (1.6 W/cm^2) wavelengths will be irradiated simultaneously onto the inner surface of clinical endoscope channels that are immersed in a GA solution (0.5%) to enhance disinfection performance and to shorten the treatment time. Moreover, Gram-positive bacteria seem more susceptible to antimicrobial agents than Gram-negative bacteria, due to the existence of an additional phospholipid layer as an outer membrane of Gram-negative strains [43]. To broaden the usage of the opto-chemical disinfection, the proposed method will be validated with various bacterial biofilms (both Gram-positive and Gram-negative bacteria).

5. Conclusion

The current results demonstrate, for the first time, the feasibility of a combined opto-chemical method for HLD of mature bacterial biofilm grown in a Teflon-based endoscope channel model. Both irreversible protein denaturation and production of intracellular ROS are responsible for approximately 1.0-$\log_{10}$ higher bacterial reduction, compared to the standard treatment. Further studies will demonstrate a capacity of the simultaneous opto-chemical treatment in disrupting biofilms of Gram positive/negative bacteria in a clinical endoscope.

Disclosures. The authors declare no conflicts of interest. A patent on the opto-chemical disinfection technology has been granted as US 10,780,187 B2 and is titled "Apparatus and method for sterilizing internal channel surface of endoscope" (H.W.K.).

Data availability. Data underlying the results presented in this paper are not publicly available at this time but may be obtained from the authors upon reasonable request.

References

1. S. Han, "Achieving competence in endoscopy," ACG Case Rep. J. **6**, e00155 (2019).
2. A. F. Peery, S. D. Crockett, C. C. Murphy, J. L. Lund, E. S. Dellon, J. L. Williams, E. T. Jensen, N. J. Shaheen, A. S. Barritt, and S. R. J. G. Lieber, "Burden and cost of gastrointestinal, liver, and pancreatic diseases in the United States: update 2018," Gastroenterology **156**(1), 254–272.e11 (2019).
3. E. Teirlinck, R. Xiong, T. Brans, K. Forier, J. Fraire, H. Van Acker, N. Matthijs, R. De Rycke, S. C. De Smedt, and T. J. N. C. Coenye, "Laser-induced vapour nanobubbles improve drug diffusion and efficiency in bacterial biofilms," Nat. Commun. **9**(1), 4518 (2018).
4. V. Molloy-Simard, J.-L. Lemyre, K. Martel, and B. J. Catalone, "Elevating the standard of endoscope processing: terminal sterilization of duodenoscopes using a hydrogen peroxide–ozone sterilizer," Am. J. Infect. Control **47**(3), 243–250 (2019).
5. H. Li, P. Torab, and P. K. Wong, "Detection of bacterial infection via a fidget spinner," Nat. Biomed. Eng. **4**, 577–578 (2020).
6. S. Hussain, J. Joo, J. Kang, B. Kim, G. B. Braun, Z.-G. She, D. Kim, A. P. Mann, T. Mölder, and T. J. N. B. E. Teesalu, "Antibiotic-loaded nanoparticles targeted to the site of infection enhance antibacterial efficacy," Nat. Biomed. Eng. **2**, 95–103 (2018).
7. P. Wang, T. Xu, S. Ngamruengphong, M. A. Makary, A. Kalloo, and S. J. G. Hutfless, "Rates of infection after colonoscopy and osophagogastroduodenoscopy in ambulatory surgery centres in the USA," Gut **67**, 1626–1636 (2018).
8. S. Park, J. Y. Jang, J. S. Koo, J. B. Park, Y. J. Lim, S. J. Hong, S.-W. Kim, H. J. Chun, D. M. Committee, K. S. o, and G. Endoscopy, "A review of current disinfectants for gastrointestinal endoscopic reprocessing," Clin. Endosc. **46**(4), 337–341 (2013).
9. V. Chandrasekhara, B. J. Elmunzer, M. Khashab, and V. R. Muthusamy, *Clinical Gastrointestinal Endoscopy E-Book* (Elsevier Health Sciences, 2018).
10. P. V. McGucken and W. Woodside, "Studies on the mode of action of glutaraldehyde on *Escherichia coli*," J. Appl. Microbiol. **36**, 419–426 (1973).
11. S. P. Committee, "Guideline for use of high-level disinfectants and sterilants for reprocessing flexible gastrointestinal endoscopes," Gastroenterol. Nurs. **38**, 70–80 (2015).
12. C. L. Ofstead, M. R. Quick, J. E. Eiland, and S. J. Adams, "A glimpse at the true cost of reprocessing endoscopes," IAHCSMM (2017).
13. M. J. E. I. O. Ciocîrlan, "Low-cost disposable endoscope: pros and cons," Endosc Int Open **07**(09), E1184–E1186 (2019).
14. K. Rupel, L. Zupin, G. Ottaviani, I. Bertani, V. Martinelli, D. Porrelli, S. Vodret, R. Vuerich, D. P. da Silva, and R. J. N. B. Bussani, and Microbiomes, "Blue laser light inhibits biofilm formation in vitro and in vivo by inducing oxidative stress," NPJ Biofilms Microbiomes **5**(1), 29 (2019).
15. G. Ş. Kaya, M. Kaya, N. Gürsan, E. Kireççi, M. Güngörmüş, H. J. P. Balta, and L. surgery, "The use of 808-nm light therapy to treat experimental chronic osteomyelitis induced in rats by methicillin-resistant *Staphylococcus aureus*," Photomed. Laser Surg. **29**(6), 405–412 (2011).
16. M. Ma, X. Liu, L. Tan, Z. Cui, X. Yang, Y. Liang, Z. Li, Y. Zheng, K. W. K. Yeung, and S. J. B. S. Wu, "Enhancing the antibacterial efficacy of low-dose gentamicin with 5 minute assistance of phototherm at 50 °C," Biomater. Sci. **7**(4), 1437–1447 (2019).
17. M. Hessling, B. Spellerberg, and K. Hoenes, "Photoinactivation of bacteria by endogenous photosensitizers and exposure to visible light of different wavelengths–a review on existing data," FEMS Microbiol. Lett. **364**(2), fnw270 (2017).
18. B. A. Barth, S. Banerjee, Y. M. Bhat, D. J. Desilets, K. T. Gottlieb, J. T. Maple, P. R. Pfau, D. K. Pleskow, U. D. Siddiqui, and J. L. J. G. E. Tokar, "Equipment for pediatric endoscopy," Gastrointest. Endosc. **76**(1), 8–17 (2012).
19. H.-C. Flemming, T. R. Neu, and D. J. Wozniak, "The EPS matrix: the "house of biofilm cells,"," J. Bacteriol. **189**(22), 7945–7947 (2007).
20. V. N. Tran, C. Dasagrandhi, V. G. Truong, Y.-M. Kim, and H. W. Kang, "Antibacterial activity of Staphylococcus aureus biofilm under combined exposure of glutaraldehyde, near-infrared light, and 405-nm laser," PLoS One **13**, e0202821 (2018).
21. M. Hull, A. Beane, J. Bowen, and C. J. A. P. Settle, and therapeutics, "Methicillin-resistant *Staphylococcus aureus* infection of percutaneous endoscopic gastrostomy sites," Aliment. Pharmacol. Ther. **15**(12), 1883–1888 (2001).
22. L. E. Murdoch, M. Maclean, E. Endarko, S. J. MacGregor, and J. G. Anderson, "Bactericidal effects of 405 nm light exposure demonstrated by inactivation of Escherichia, Salmonella, Shigella, Listeria, and Mycobacterium species in liquid suspensions and on exposed surfaces," Sci. World J. **2012**, 137805 (2012).

23. L. Pineau, C. Roques, J. Luc, and G. Michel, "Automatic washer disinfector for flexible endoscopes: a new evaluation process," Endoscopy **29**(05), 372–379 (1997).
24. C. Aumeran, E. Thibert, F. Chapelle, C. Hennequin, O. Lesens, and O. Traore, "Assessment on experimental bacterial biofilms and in clinical practice of the efficacy of sampling solutions for microbiological testing of endoscopes," J. Clin. Microbiol. **50**(3), 938–942 (2012).
25. F. Khan, J.-W. Lee, P. Manivasagan, D. T. N. Pham, J. Oh, and Y.-M. J. M. P. Kim, "Synthesis and characterization of chitosan oligosaccharide-capped gold nanoparticles as an effective antibiofilm drug against the *Pseudomonas aeruginosa* PAO1," Microb. Pathog. **135**, 103623 (2019).
26. V. N. Tran, H. Lee, V. G. Truong, Y. H. Rhee, and H. W. Kang, "Concentric photothermal coagulation with basket-integrated optical device for treatment of tracheal stenosis," J. Biophotonics **11**, e201700073 (2017).
27. W. A. Rutala and D. J. Weber, "Disinfection and sterilization: an overview," Am. J. Infect. Control. **41**(5), S2–S5 (2013).
28. R. K. Saroj, K. N. Murthy, and M. Kumar, "Nonparametric statistical test approaches in genetics data," Int. J. Comput. Biol. **5**(1), 77–87 (2015).
29. G. W. Divine, H. J. Norton, A. E. Barón, and E. Juarez-Colunga, "The Wilcoxon–Mann–Whitney procedure fails as a test of medians," AM STAT **72**(3), 278–286 (2018).
30. J. Y. Maillard, "Bacterial target sites for biocide action," J. Appl. Microbiol. **92**, 16S–27S (2002).
31. Q. Li, B.-J. Lee, Z. M. Zhang, and D. W. Allen, "Light scattering of semitransparent sintered polytetrafluoroethylene films," J. Biomed. Opt. **13**(5), 054064 (2008).
32. N. Huber, J. Heitz, and D. Bäuerle, "Pulsed-laser ablation of polytetrafluoroethylene (PTFE) at various wavelengths," Eur. Phys. J. Appl. Phys. **25**(1), 33–38 (2004).
33. T. Kamai, G. J. Kluitenberg, and J. W. Hopmans, "A dual-probe heat-pulse sensor with rigid probes for improved soil water content measurement," Soil Sci. Soc. Am. J. **79**(4), 1059–1072 (2015).
34. D. X. Zhang, R. Zhang, Z. He, J. J. Wu, and F. Zhang, "Numerical Investigation on Laser Ablation Characteristics of PTFE in Advanced Propulsion Systems," in *Appl. Mech. Mater.* (Trans Tech Publ, 2012), 727–731.
35. J.-W. Ha and D.-H. Kang, "Simultaneous near-infrared radiant heating and ultraviolet radiation for inactivating *Escherichia coli* O157: H7 and *Salmonella enterica* serovar Typhimurium in powdered red pepper (*Capsicum annuum* L.)," Appl. Environ. Microbiol. AEM. **1**, 02249–02213 (2013).
36. P. Ramakrishnan, M. Maclean, S. J. MacGregor, J. G. Anderson, and M. H. Grant, "Cytotoxic responses to 405 nm light exposure in mammalian and bacterial cells: Involvement of reactive oxygen species," Toxicol In Vitro. **33**, 54–62 (2016).
37. J. Fyrestam, N. Bjurshammar, E. Paulsson, A. Johannsen, C. J. A. Östman, and B. Chemistry, "Determination of porphyrins in oral bacteria by liquid chromatography electrospray ionization tandem mass spectrometry," Anal. Bioanal. Chem. **407**(23), 7013–7023 (2015).
38. FDA, "Infections Associated with Reprocessed Duodenoscopes," (2019).
39. S. Bhatt, P. Mehta, C. Chen, C. L. Schneider, L. N. White, H.-L. Chen, and M. G. Kong, "Efficacy of low-temperature plasma-activated gas disinfection against biofilm on contaminated GI endoscope channels," Gastrointest. Endosc. **89**(1), 105–114 (2019).
40. W. A. Rutala and D. J. Weber, "Guideline for disinfection and sterilization in healthcare facilities, 2008," CDC, 1–161 (2008).
41. M. S. Neves, M. G. da Silva, G. M. Ventura, P. B. Côrtes, R. S. Duarte, and H. S. de Souza, "Effectiveness of current disinfection procedures against biofilm on contaminated GI endoscopes," Gastrointest. Endosc. **83**(5), 944–953 (2016).
42. A. C. Balsamo, K. U. Graziano, R. P. Schneider, M. Antunes Junior, and R. A. Lacerda, "Removing biofilm from a endoscopic: evaluation of disinfection methods currently used," Rev. esc. enferm. USP **46**(spe), 91–98 (2012).
43. I. W. Fong, D. Shlaes, and K. Drlica, *Antimicrobial Resistance in the 21st Century* (Springer, 2018).